World Journal of Engineering Research
Print ISSN: 2959-9865
Online ISSN: 2959-9873
DOI: https://doi.org/10.61784/wjer3046

STRUCTURAL DESIGN AND KINEMATIC ANALYSIS OF A BIONIC FROG JUMPING ROBOT

Peng Zhang*, XinYue Zhou
School of Mechanical Engineering, Chengdu University, Chengdu 610106, Sichuan, China.
Corresponding Author: Peng Zhang, Email: zhangpeng@cdu.edu.cn

Abstract: Jumping robots have garnered significant attention from both academia and industry due to their superior obstacle negotiation capabilities and high mobility. The bionic frog-inspired jumping robot represents a pivotal research focus within this domain. This study initiates with a biological examination of frogs, identifying two critical factors governing their jumping performance: center-of-gravity adjustment and hindlimb movement. A simplified structural model of the frog is established to inform the structural design of the bionic robot. The kinematic analysis is then prioritized, specifically targeting the jumping actuation mechanism. An analytical method is employed to develop a mathematical model of the mechanism, investigating the patterns of its output displacement, velocity, and acceleration. MATLAB simulations are conducted to generate motion sequence diagrams of the mechanism and the curves illustrating the angular displacement, angular velocity, and angular acceleration of each linkage. The results validate the rationality and feasibility of the mechanism's design, thereby laying a theoretical foundation for subsequent structural optimization efforts.
Keywords: Bionic frog robot; Structural design; Kinematic analysis; Jumping mechanism

1 INTRODUCTION

Increasingly mature robotics technology demonstrates significant potential and impact across numerous industries, promising broad prospects for development and application in both present and future markets. As robotics technology becomes widely adopted in various fields, its application scope continues to expand, with future potential extending to extreme environments such as space exploration and deep-sea investigation [1-2]. When tasked with exploring such unknown environments, although mobile robots with high stability and strong load capacity show considerable adaptability, they often struggle to effectively traverse complex terrain. Seeking alternative paths tends to increase both mission duration and operational difficulty. To address these challenges, the concept of jumping robots has emerged [3-4].

This paper takes the frog as a bionic research target to develop a jumping robot with outstanding obstacle-crossing performance, excellent mobility, and strong adaptability to complex terrain, thereby addressing the limitations of traditional mobile robots in terms of movement flexibility and environmental adaptability. Through in-depth analysis of the frog's movement mechanisms, this study aims to reveal general principles of biological jumping motion. A simplified structural model of the frog will be constructed to guide the structural design of the bionic frog jumping robot. Furthermore, an analytical method will be applied to perform kinematic analysis of its jumping mechanism, with a focus on investigating its motion characteristics.

2 STRUCTURAL DESIGN OF THE BIONIC FROG

In the field of bionics, the frog has become an ideal subject for biomimetic research due to its exceptional jumping ability, providing key insights for the design of jumping robots. This section begins by analyzing the frog's movement mechanisms, then constructs a simplified structural model, and finally carries out the structural design of the bionic frog jumping robot.

2.1 Movement Mechanism of the Frog

2.1.1 Structural characteristics of the frog

From an anatomical perspective, the morphological features of the frog are mainly reflected in its skeletal system and muscular tissue. The frog's body structure can be divided into three main parts: the forelimbs, the trunk, and the hindlimbs. The biological characteristics of the forelimbs and hindlimbs are key focuses of structural research.

An analysis of the anatomical structure reveals that the limb skeletal system of frogs exhibits distinct regional characteristics: the forelimb bones, from proximal to distal, include the humerus, radioulna, carpals, metacarpals, and phalanges; the hindlimb skeletal system consists of the femur, tibiofibula, tarsals, metatarsals, and phalanges. The humerus and radioulna of the forelimbs are approximately equal in length, and a similar proportional relationship exists between the femur and tibiofibula in the hindlimbs. In terms of motor function, the phalanges serve as the end-support structures and play a major supportive role during jumping. A lateral view of the frog skeleton is shown in Figure 1 [5]. Regarding the joint system, the forelimb kinematic chain consists of the shoulder, elbow, and wrist joints, while the

hindlimb relies on a compound motion system formed by the hip, knee, ankle, and tarsometatarsal joints. A top view of the frog joints is shown in Figure 2 [6].

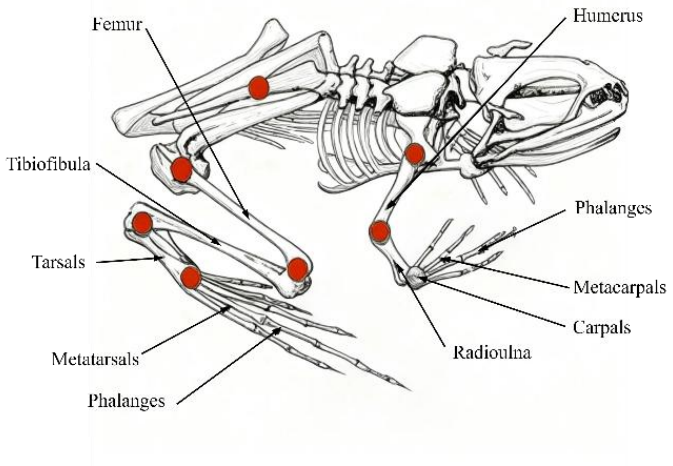

Figure 1 Side View of a Frog's Skeleton

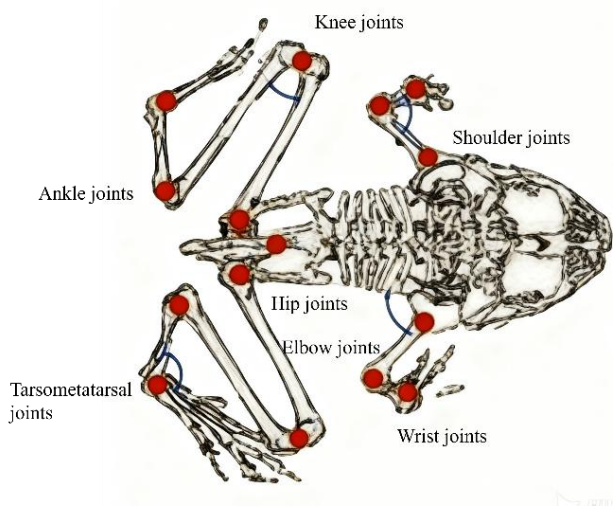

Figure 2 Top View of the Frog's Joints

Observation and analysis of the frog's movement mechanism indicate that the forelimbs primarily provide support during jumping, while the hindlimb muscles serve as the power source and key structure for motion control. Based on this biomechanical characteristic, this study focuses on the morphology and function of the hindlimb muscle groups. Anatomical studies show that the frog's hindlimb muscular system mainly consists of the gluteus, semimembranosus, biceps femoris, and gastrocnemius, among others. The detailed anatomical structure can be referred to in Figure 3 [7].

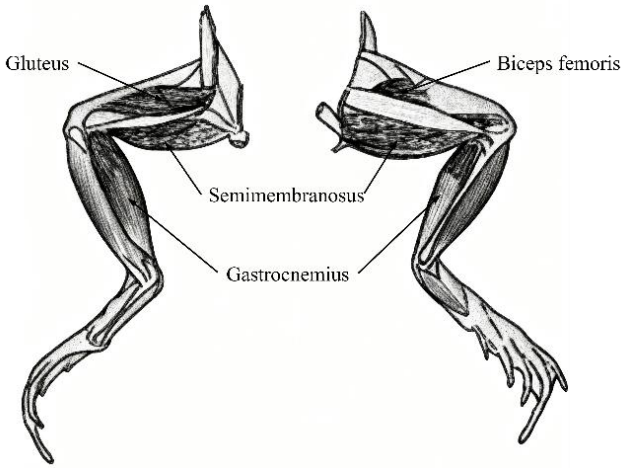

Figure 3 The Diagram of the Hind Limb Muscles of a Frog

2.1.2 Jumping process of the frog

The complete jumping cycle of a frog consists of three main phases, as shown in Figure 4: take-off, aerial, and landing [8]. The body posture during the landing phase highly resembles the initial take-off posture, indicating that the jumping cycle forms a closed loop. Analysis of the frog's jumping motion reveals that the key factors influencing take-off are center of gravity adjustment and hindlimb movement. During the preparatory phase, the frog actively lowers its overall center of gravity to optimize take-off posture. Subsequently, the hindlimb muscles undergo rapid concentric contraction to release energy. This explosive contraction generates substantial ground reaction force, which is the core biological factor determining the dynamic performance during take-off.

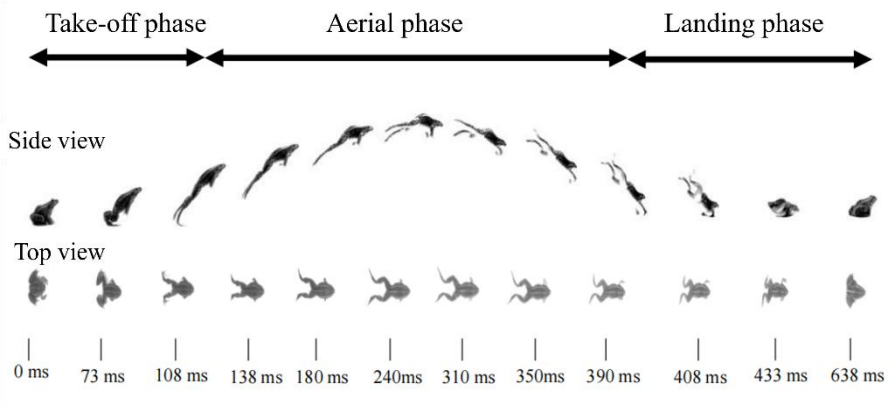

Figure 4 Diagram of the Frog's Jumping Process

2.2 Simplified Structural Model of the Frog

Based on the study and analysis of the frog's movement mechanism, its physiological structure was reasonably simplified to establish a simplified structural model, as shown in Figure 5. This model serves as the basis for the structural design and modeling of the bionic frog.

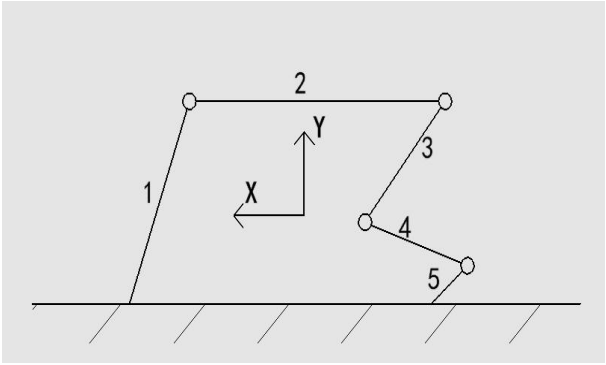

Figure 5 Simplified Model Diagram of the Frog Structure

In the figure, Component 1 represents the forelimb structure, which primarily provides support. Component 2 represents the trunk, designed to be longer than the forelimbs. The thigh and shank of the hindlimb are represented by Components 3 and 4, respectively, with the thigh segment being slightly longer than the shank. Component 5 represents the toe structure at the end of the hindlimb.

2.3 Structural Design and Modeling of the Bionic Frog

2.3.1 Transmission system design

This paper adopts a composite driving scheme combining an electric motor and a spring. The specific design of the drive system is shown in Figure 6.

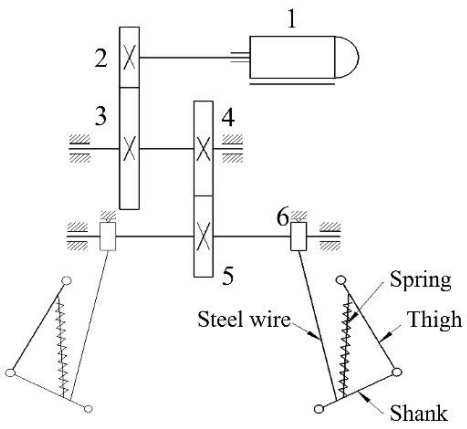

Figure 6 Schematic Diagram of the Drive System

In the transmission system, Component 1 is the drive motor; Components 2, 3, and 5 are standard spur gears; Component 4 is a missing-tooth gear; and Component 6 is a drum, which is directly connected to the jumping mechanism via a steel wire.

The transmission process is as follows: the torque generated by the drive motor 1 is transmitted via gear 2 on its shaft to the meshing gear 3. The missing-tooth gear 4, which is coaxial with gear 3, engages with and drives gear 5. The drum rotates coaxially with gear 5. As the drum rotates around its axis, the steel wire is wound up, stretching the shank and compressing the energy-storing spring. Once the missing-tooth gear 4 completes its engagement cycle with gear 5, the meshing relation is abruptly disengaged. This causes the shaft carrying gear 5 and the drum to reverse rotation, allowing the compressed spring to release rapidly and ultimately execute the jump.

2.3.2 Jumping mechanism design

During the frog's jump, the hind legs perform the primary jumping function. To effectively simulate the frog's jumping posture and achieve jumping performance, this study designed the jumping mechanism of the bionic frog based on the hind leg posture during take-off. The final design is a multi-bar mechanism with one degree of freedom, as shown in Figure 7, where segment HI represents the compressible spring. This design facilitates control of the take-off angle and effectively simulates the posture change of the frog's hind legs during jumping.

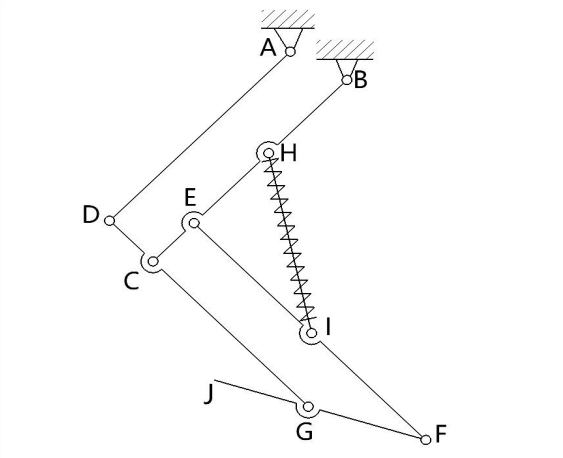

Figure 7 Simplified Diagram of the Jumping Actuator

2.3.3 Mechanical system assembly model

After determining the key parameters of the transmission system and the jumping mechanism, the geometric dimensions of each component, the configuration of transmission shafts and their support structures, assembly relationships, and axial constraints and connection methods were designed and selected according to overall design specifications. The final assembly model is shown in Figure 8.

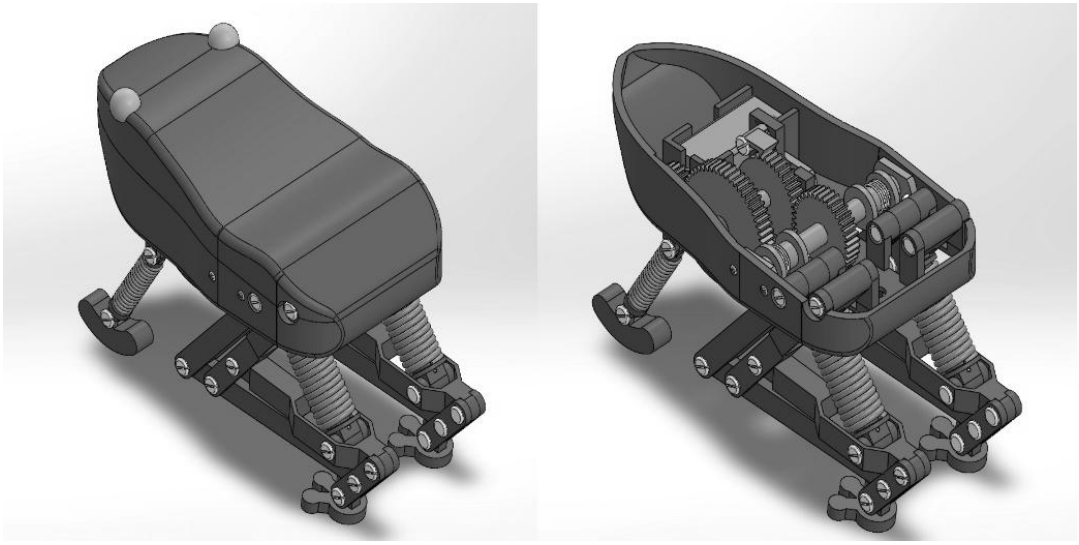

Figure 8 Bionic Frog Assembly Model

3 KINEMATIC ANALYSIS OF THE JUMPING MECHANISM

The hind limb is the core component enabling the jumping function of the overall system, and its kinematic characteristics are the main focus of this analysis. Based on the simplified model shown in Figure 9, this section employs an analytical method to conduct position, velocity, and acceleration analyses of each linkage.

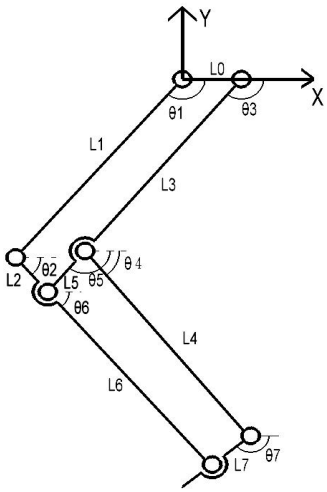

Figure 9 Analysis Model of the Jumping Actuator

For this six-bar mechanism, the kinematic properties can be derived by constructing two vector loop equations based on a four-bar linkage model. In this process, the output angular displacement is determined by solving the two vector loops sequentially. The displacement output from the first four-bar vector loop serves as the input parameter for the second loop. This recursive relationship accurately models the kinematic correlations among the components of the mechanism [5].

3.1 Position Analysis

In the figure, L_0-L_7 represent the lengths of the linkages, all of which are known. θ_1-θ_6 denote the orientation angles of each link, with θ_1 defined as the input angle. Vectors $\boldsymbol{l_0}$-$\boldsymbol{l_7}$ correspond to each linkage. The first vector loop satisfies the following vector relation:

$$\boldsymbol{l}_1+\boldsymbol{l}_2=\boldsymbol{l}_3+\boldsymbol{l}_0 \tag{1}$$

Rewritten in complex vector form:

$$L_1e^{i\theta_1}+L_2e^{i\theta_2}=L_3e^{i\theta_3}+L_0 \tag{2}$$

Using Euler's formula to expand the expression and separating the real and imaginary parts yields the following equations:

$$\begin{cases} &L_1 \cos\theta_1 + L_2 \cos\theta_2 = L_3 \cos\theta_3 + L_0 \\ &L_1 \sin\theta_1 + L_2 \sin\theta_2 = L_3 \sin\theta_3 \end{cases} \tag{3}$$

Solving the system of equations gives:

$$\theta_3 = 2\arctan\frac{-A \pm \sqrt{A^2+B^2-C^2}}{B+C} \tag{4}$$

$$\theta_2 = 2\arctan\frac{D \pm \sqrt{D^2+E^2-F^2}}{E+F} \tag{5}$$

where $A=2L_1L_3\sin\theta_1$, $B=2L_3(L_1\cos\theta_1+L_0)$, $C=L_2^2-L_1^2-L_3^2-L_0^2+2L_1L_0\cos\theta_1$, $D=2L_1L_2\sin\theta_1$, $E=2L_2(L_1\cos\theta_1-L_0)$, $F=L_3^2-L_1^2-L_2^2-L_0^2+2L_1L_0\cos\theta_1$.

Similarly, using the output parameters from the first vector loop $\theta_3=\theta_5$ and $\theta_2=\theta_6$—as known inputs, the same analytical method is applied to solve for the output angles θ_4 and θ_7 of the second vector loop:

$$\theta_4 = 2\arctan\frac{G \pm \sqrt{G^2+H^2-I^2}}{H+I} \tag{6}$$

$$\theta_7 = 2\arctan\frac{J \pm \sqrt{J^2+K^2-L^2}}{K+L} \tag{7}$$

where $G=2L_4(L_5\sin\theta_5-L_6\sin\theta_6)$, $H=2L_4(L_5\cos\theta_5-L_6\cos\theta_6)$, $I=L_7^2-L_4^2-L_5^2-L_6^2+2L_5L_6\cos(\theta_5-\theta_6)$, $G=2L_4(L_5\sin\theta_5-L_6\sin\theta_6)$, $H=2L_4(L_5\cos\theta_5-L_6\cos\theta_6)$, $I=L_7^2-L_4^2-L_5^2-L_6^2+2L_5L_6\cos(\theta_5-\theta_6)$.

Each of the equations (4) to (7) yields two possible solutions for the angles. The appropriate sign (positive or negative) should be selected based on the actual configuration.

3.2 Velocity Analysis

The angular velocity equations are derived by differentiating the position equations. Differentiating equation (2) with respect to time *t* gives:

$$L_1\omega_1 e^{i\theta_1} + L_2\omega_2 e^{i\theta_2} = L_3\omega_3 e^{i\theta_3} \tag{8}$$

Separating the real and imaginary parts of the above equation results in two independent equations. Solving these simultaneously yields the numerical values of the unknown angular velocities ω_2 and ω_3:

$$\omega_3 = \frac{\omega_1 l_1 \sin(\theta_1-\theta_2)}{l_3 \sin(\theta_3-\theta_2)} \tag{9}$$

$$\omega_2 = -\frac{\omega_1 l_1 \sin(\theta_1-\theta_3)}{l_2 \sin(\theta_2-\theta_3)} \tag{10}$$

Similarly, the two unknown angular velocities of the second vector loop, ω_4 and ω_7, can be obtained:

$$\omega_4 = \frac{\omega_6 l_6 \sin(\theta_6-\theta_7)}{l_4 \sin(\theta_4-\theta_7)} \tag{11}$$

$$\omega_7 = \frac{\omega_6 l_6 \sin(\theta_6-\theta_4)}{l_7 \sin(\theta_7-\theta_4)} \tag{12}$$

3.3 Acceleration Analysis

The angular acceleration equations are derived by differentiating the angular velocity equations. Differentiating equation (8) with respect to time t gives:

$$iL_1\omega_1^2 e^{i\theta_1} + L_2\alpha_2 e^{i\theta_2} + iL_2\omega_2^2 e^{i\theta_2} = L_3\alpha_3 e^{i\theta_3} + iL_3\omega_3^2 e^{i\theta_3} \tag{13}$$

Separating the real and imaginary parts and solving the system of equations yields the numerical values of the unknown angular accelerations α_2 and α_3:

$$\alpha_3 = \frac{\omega_1^2 l_1 \cos(\theta_1-\theta_2) + \omega_2^2 l_2 - \omega_3^2 l_3 \cos(\theta_3-\theta_2)}{l_3 \sin(\theta_3-\theta_2)} \tag{14}$$

$$\alpha_2 = \frac{-\omega_1^2 l_1 \cos(\theta_1-\theta_3) - \omega_2^2 l_2 \cos(\theta_2-\theta_3) + \omega_3^2 l_3}{l_2 \sin(\theta_2-\theta_3)} \tag{15}$$

Similarly, the two unknown angular accelerations of the second vector loop, α_4 and α_7, can be determined:

$$\alpha_4 = \frac{-\omega_6^2 l_6 \cos(\theta_6-\theta_7) + \omega_7^2 l_7 - \omega_4^2 l_4 \cos(\theta_4-\theta_7)}{l_4 \sin(\theta_4-\theta_7)} \tag{16}$$

$$\alpha_7 = \frac{\omega_6^2 l_6 \cos(\theta_6-\theta_4) + \omega_4^2 l_4 - \omega_7^2 l_7 \cos(\theta_7-\theta_4)}{l_7 \sin(\theta_7-\theta_4)} \tag{17}$$

Using the above methods and equations, the position, velocity, and acceleration parameters of each linkage in the jumping mechanism can be obtained, thereby clarifying its kinematic characteristics.

4 MATLAB SIMULATION ANALYSIS

Following the kinematic analysis of the jumping mechanism, a simulation was conducted using Matlab to establish a mathematical model based on the kinematic results, in order to verify whether the mechanism can achieve the designed jumping motion.

4.1 Simulation of Mechanism Motion Posture

The rocker of the mechanism was discretized into multiple rotation nodes at equal intervals. Based on the results of the kinematic position analysis, the corresponding joint angles and positions of the mechanism at each discrete point were

solved. The mechanism positions were then simulated using Matlab's plotting function, as shown in Figure 10. It can be observed that the motion posture change of the jumping mechanism closely matches the hind leg movement of a frog during an actual jump.

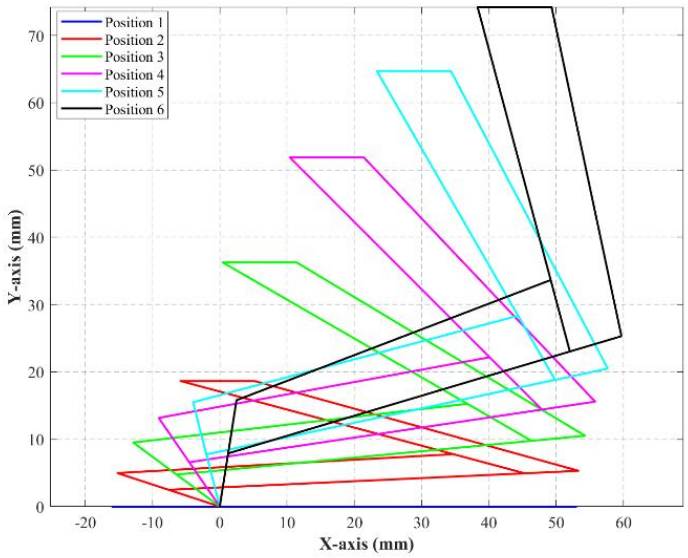

Figure 10 Diagram of the Change in the Motion Posture of the Jumping Actuator

4.2 Simulation of Kinematic Analysis Results

The expressions for the position, velocity, and acceleration of each linkage derived from the kinematic analysis were simulated using Matlab's plotting functionality. The simulation results are shown in Figures 11 to 13. The curves indicate that the angular displacement of each linkage changes smoothly without abrupt transitions over a full motion cycle. The variations in angular velocity and angular acceleration remain within reasonable ranges, demonstrating relatively stable operation of the mechanism. These results validate the feasibility of the jumping execution mechanism.

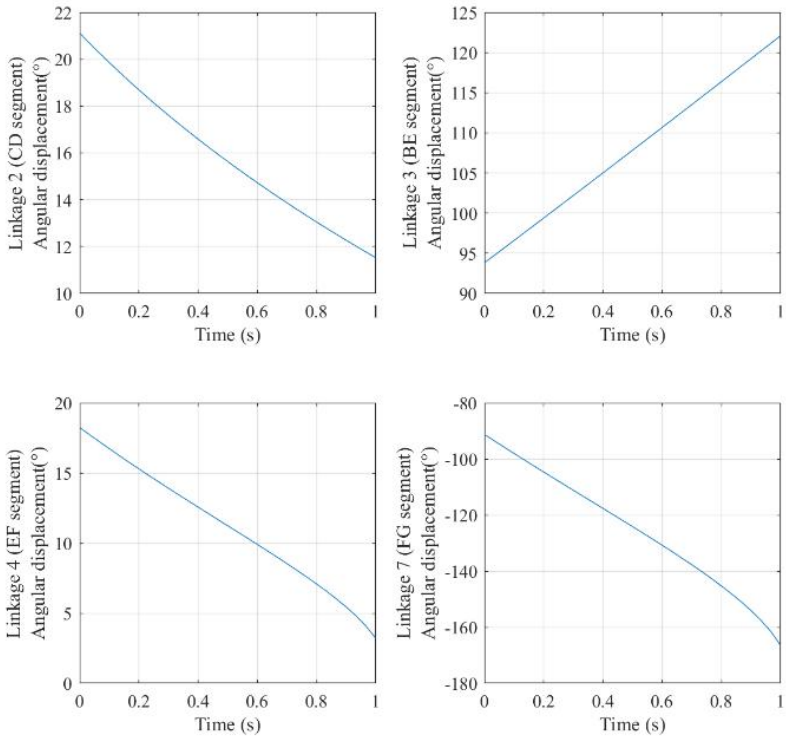

Figure 11 Diagram of Angular Displacement Changes of Each Linkage

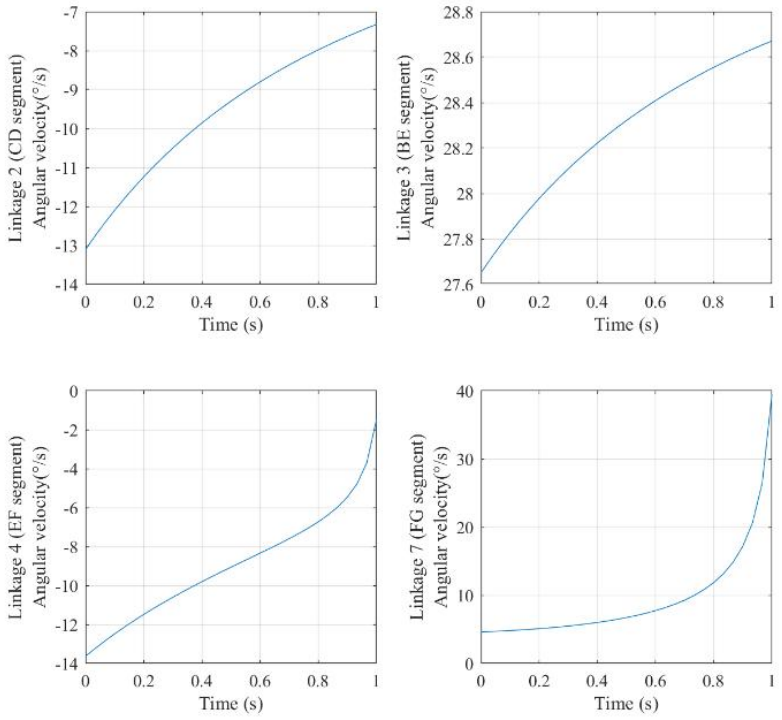

Figure 12 Diagram of Angular Velocity Changes of Each Linkage

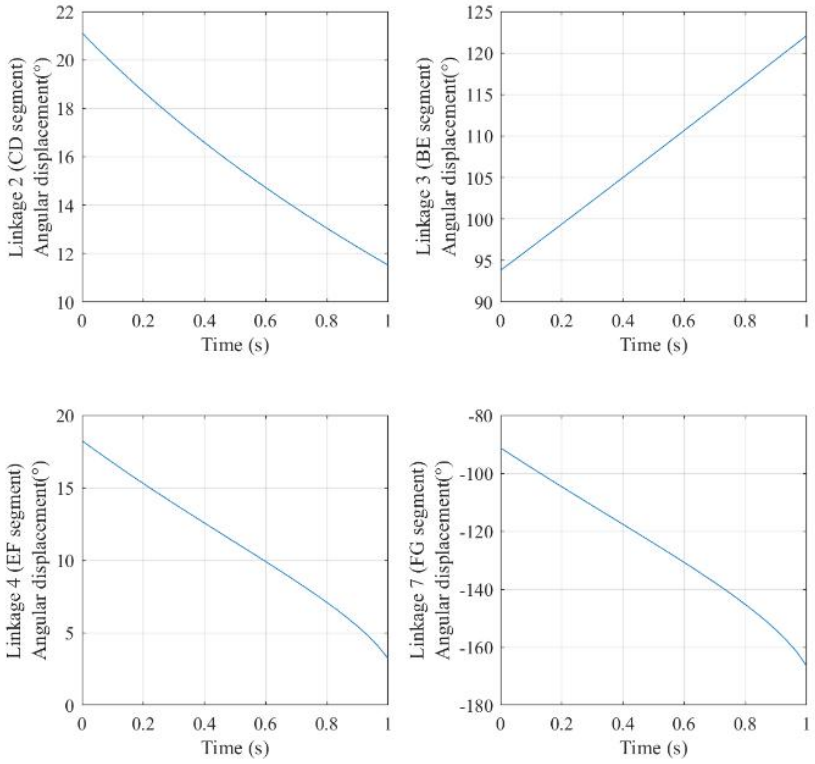

Figure 13 Diagram of Angular Acceleration Changes of Each Linkage

5 CONCLUSION

This study analyzed the movement mechanism of frogs to develop a simplified structural model, which led to the structural design of a bionic frog robot. Particular emphasis was placed on the design of the transmission system and the jumping mechanism. Kinematic analysis was conducted on the core jumping mechanism to determine the displacement,

velocity, and acceleration patterns of each linkage. Furthermore, Matlab simulation software was employed to visualize the kinematic behavior of the mechanism. The resulting motion posture diagrams and parameter variation curves validated the feasibility and rationality of the proposed mechanism, thereby laying a theoretical foundation for subsequent structural optimization.

COMPETING INTERESTS

The authors have no relevant financial or non-financial interests to disclose.

FUNDING

This research was supported by Natural Science Foundation of Sichuan Province (Grant No. 2023NSFSC0368), Talents Project of Chengdu University (Grant No. 2081921013)

REFERENCES

[1] Men B, Fan X K, Chen Y X. Research status and development trends of bionic robots. Robot Technology and Application, 2019(5): 15-19.
[2] Lo J, Parslew B. Characterising the take-off dynamics and energy efficiency in spring-driven jumping robots. Mechanism and Machine Theory, 2024, 199. DOI: 10.1016/j.mechmachtheory.2024.105688.
[3] Tang G, Yang Q, Lian B. Design and Experimentation of Tensegrity Jumping Robots.Applied Sciences-Basel, 2024, 14(9): 18. DOI: 10.3390/app14093947.
[4] Wang G B, Chen D S, Chen KW, et al. Research status and development trends of bionic robots. Journal of Mechanical Engineering, 2015, 51(13): 27-44.
[5] Gu Y C. Design and research of a bionic frog jumping robot. Dalian Jiaotong University, 2021.
[6] Wang M. Development of a bionic frog jumping robot. Harbin Institute of Technology, 2011.
[7] Lei B J. Kinematic simulation and landing impact process analysis of a bionic frog hopping robot. Zhejiang Sci-Tech University, 2017.
[8] Lin F. Research on a posture adjustment device imitating the aerial movement patterns of frog hindlimbs. Harbin Institute of Technology, 2022.